SIZE EFFECT IN PENETRATION OF SEA ICE PLATE WITH PART-THROUGH CRACKS. I: THEORY

By Zdeněk P. Bažant,[1] Fellow, ASCE, and Jang Jay H. Kim[2]

ABSTRACT: The paper analyzes the vertical penetration of a small object through a floating sea ice plate. The analysis takes into account the fact that the bending cracks reach only through part of the ice plate thickness and have a variable depth profile. The cracks are modeled according to the Rice-Levy nonlinear softening line spring model. The plate-crack interaction is characterized in terms of the compliance functions for the bending moments and normal forces in the crack plane, which are computed by an energy-based variational finite-difference method. The radial crack is divided into vertical strips, and a numerical algorithm with step-by-step loading is developed to calculate the vertical growth of the crack in each strip for a prescribed radial crack length increment. The initiation of crack strips from the surface of the plate is decided on the basis of a yield strength criterion with a fracture based flow rule. Systems of up to 300 nonlinear equations are solved by the Levenberg-Marquardt optimization algorithm. The maximum load is reached when the circumferential cracks begin to form. Numerical calculations, comparison of the results with test data, and a study of scaling laws are relegated to the companion paper, which follows in this issue. Numerical calculations show a typical quasi brittle size effect such that the plot of log σ_N versus log h (where σ_N = nominal stress at maximum load and h = plate thickness) is a descending curve whose slope is negligible only for $h < 0.2$ m and then gets gradually steeper, asymptotically approaching $-1/2$. The calculated size effect agrees with the existing test data, and contradicts previous plasticity solutions.

INTRODUCTION

Sea ice plates subjected to a vertical load applied on a small area from above or below typically fail by propagation of radial cracks in a star pattern [Fig. 1(a)]. The maximum load, which represents the failure load under load control conditions, is reached when circumferential cracks start to form (Frankenstein 1963).

The penetration problem is important for many operations in the Arctic Ocean such as airplanes landing on the ice, vehicles traveling on the ice, or submarines penetrating through the ice from below. Of particular interest is the size effect on the nominal strength, which governs extrapolation of small-scale laboratory tests to such field situations.

The problem has been studied extensively for a long time (Bernstein 1929; Frankenstein 1963, 1966; Kerr 1975, 1996). Because small-scale laboratory tests show sea ice to be notch insensitive, the applicability of fracture mechanics to sea ice has been doubted for a long time. So it is not surprising that the penetration problem had until recently been analyzed on the basis of the strength criterion and plastic limit analysis (Kerr 1996). However, the doubts started to dissipate after Dempsey (1989, 1990; DeFranco and Dempsey 1990) suggested that this conclusion was due merely to insufficient size of the specimens. The applicability of fracture mechanics to sea ice on a large scale has recently been demonstrated by the in-situ experiments of Dempsey and coworkers (Adamson et al. 1995; Dempsey et al. 1995a,b; Dempsey 1996; Mulmule et al. 1995; Mulmule and Dempsey 1997).

In the early studies, the load capacity of a floating sea ice plate was determined by elastic analysis coupled with the tensile strength criterion (Bernstein 1929). Nevel (1958) used the strength criterion, assuming that there is a large number of radial bending cracks splitting the ice plate into small-angle wedges that can be treated as beams of variable cross section.

Sea ice, however, is a quasibrittle material which, when failing in tension, exhibits no plastic yield plateau but postpeak softening. Such behavior alone, as a matter of principle, implies the plasticity solutions to be unrealistic except for very small sizes. [For general information, see Bažant (1983, 1984, 1993); Bažant and Planas (1998). For specific information regarding sea ice, see Bažant and Kim (1985); Bažant and Gettu (1991).] From the practical viewpoint, the main limitation of plastic limit analysis is that it cannot capture the size effect on the nominal strength of the structure. Only fracture mechanics can do that. The size effect is not statistical (Bažant et al. 1991), nor fractal (Bažant 1997a,b), but is caused by the fact that, with increasing size (plate thickness, in this case), the stored and subsequently released energy increases faster than the energy consumed and dissipated by fracture. This is called the quasibrittle size effect.

An additional reason why correct solutions must be based on fracture mechanics is that the maximum load is reached only after stable growth of large cracks. In that case, a deterministic size effect due to energy released by large cracks necessarily takes place and prevails over the statistical size effect of Weibull type (Bažant et al. 1991; Bažant and Planas 1998). If the plate failed right at crack initiation, the use of fracture mechanics would not be necessary and the strength criterion might be appropriate, provided that the stress redistribution due to a microcracking zone formed before attaining the maximum load could also be neglected. In that case, which is not the real situation, the size effect of Weibull type would have to be expected (Bažant et al. 1991; Bažant 1997a,b; Bažant and Chen 1997; Bažant and Planas 1998).

Fracture mechanics has been applied to the penetration problem by Slepyan (1990), Bažant (1992a,b). Bažant and Li (1994a,b), Li and Bažant (1994), Bažant et al. (1995), and Dempsey et al. (1995a,b). To take the effect of the radial bending cracks approximately into account, linear elastic fracture mechanics (LEFM) was introduced by Bažant and Li (1994a,b). They used Nevel's (1958) one-dimensional approximation to calculate the energy release caused by radial crack propagation. Li and Bažant (1994) carried out a two-dimensional analysis and formulated a method to determine the number of initiating radial cracks.

In the aforementioned studies, the radial cracks were as-

[1]Walter P. Murphy Prof. of Civ. Engrg. and Mat. Sci., Northwestern Univ., Evanston, IL 60208. E-mail: z-bazant@nwu.edu

[2]Grad. Res. Asst., Dept. of Civ. Engrg., Northwestern Univ., Evanston, IL.

Note. Associate Editor: George V. Voyiadjis. Discussion open until May 1, 1999. Separate discussions should be submitted for the individual papers in this symposium. To extend the closing date one month, a written request must be filed with the ASCE Manager of Journals. The manuscript for this paper was submitted for review and possible publication on November 13, 1996. This paper is part of the ***Journal of Engineering Mechanics***, Vol. 124, No. 12, December, 1998. ©ASCE, ISSN 0733-9399/98/0012-1310–1315/$8.00 + $.50 per page. Paper No. 14531.

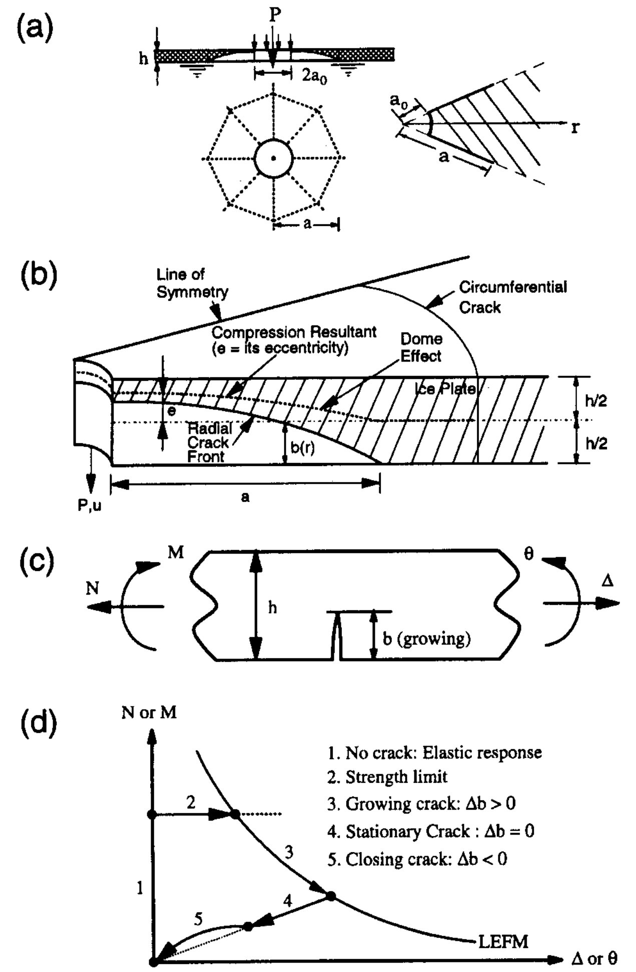

FIG. 1. Diagram of: (a) Vertical Cross Section of Floating Sea Ice Plate, Crack Pattern Viewed from Top and Plate Wedge between Two Adjacent Radial Cracks; (b) Half of Plate Wedge with Part-Through Crack Profile and Schematic Representation of Compression Resultant Elevation Showing Dome Effect; (c) Bending Moment and Normal Force Acting on Cracked Cross Section, and Additional Rotation and Displacement due to Crack; (d) Stages in Evolution of Vertical Crack Strips

sumed to be fully opened through-cracks. However, the horizontal expansion that is associated with bending cracks causes the cracks to open through only a part of the thickness of the plate, as experimentally observed by Frankenstein (1963). This expansion induces compressive forces in the plate and thus engenders a dome effect, which plays an important role in helping to carry the vertical load [see the idealized dome shape in Fig. 1(b)]. The importance of the dome effect in plates, and a similar effect in beams called the arching action, was recognized by many authors. [Regarding concrete, see Ockleston (1958); Park (1964, 1965); Desayi; and Kulkarni (1977); Park and Gamble (1980); Black (1975); Braestrup and Morley (1980). Regarding floating ice, see Sodhi (1995a,b); Kerr (1996)]. But these studies were made under the assumption of plastic behavior.

A plate with part-through cracks is actually a three-dimensional fracture problem. However, based on the simplifying idea of an embedded softening line spring, proposed by Rice and Levy (1972) in a study of the fracture of metal plates, the problem can be reduced to a two-dimensional one. Since the opening depth of the radial bending cracks is unknown in advance, the functions defining the compliances of the line springs must be solved together with the plate problem.

In the present paper, the problem will be solved by means of a system of integral equations based on the compliance functions of the floating plate wedge formed by two adjacent cracks. This formulation was given by Bažant et al. (1995), who also incorporated the nonlinear line spring model. The formulation will be extended by introducing a method to calculate the initiation of new crack segments. In a subsequent paper (Bažant and Kim 1998), a numerical solution of the problem will be obtained using a nonlinear optimization algorithm. The size effect will be analyzed and the dome effect will be demonstrated.

FLOATING PLATE WITH PART-THROUGH RADIAL CRACKS

Consider an infinitely extending elastic plate of thickness h, floating on water of specific weight ρ [Fig. 1(a)]. The water acts exactly as an elastic foundation of Winkler type. The differential equation of equilibrium of the plate in terms of the vertical downward deflection w as a function of rectangular coordinates x and y may be written as $D\nabla^4 w + \rho w = 0$, where $D = Eh^3/12(1 - \nu^2)$ = cylindrical stiffness of the plate; ν = Poisson's ratio; and E = Young's modulus. The load is assumed to be applied only on the boundary of the plate.

It is convenient to introduce a length constant for the plate, $L = (D/\rho)^{1/4}$, called the flexural wavelength. It represents the length over which an end disturbance in a semiinfinite plate decays to e^{-1} of the end value. Introducing the dimensionless coordinates $X = x/L$ and $Y = y/L$, we may rewrite the differential equation of the plate as

$$\left(\frac{\partial^2}{\partial X^2} + \frac{\partial^2}{\partial Y^2}\right)\left(\frac{\partial^2 w}{\partial X^2} + \frac{\partial^2 w}{\partial Y^2}\right) + w = 0 \tag{1}$$

The assumption of full-through cracks, however, is realistic only if the parts of the plate separated by the crack can move freely apart. This is true for a long thermal fracture in an infinite ice plate (Bažant 1992a,b), or for very thin plates. In the present problem, the plate wedge prevents the sides of the crack from moving freely apart. Thus, the relative rotations across the crack cause the top portion of the ice plate to come under horizontal compression [Fig. 1(a)]. The resultant of the in-plane compression force in the planes gets shifted above the midthickness. This engenders a dome effect (Fig. 2), which

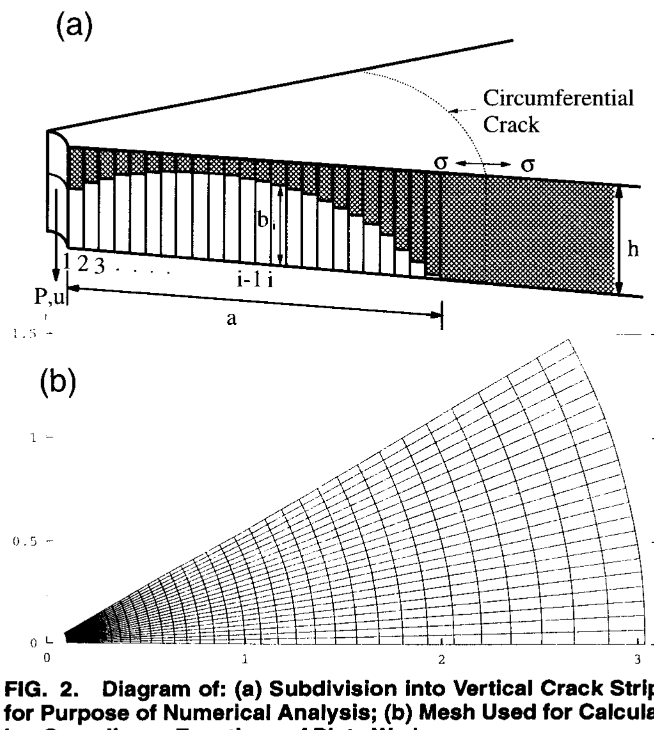

FIG. 2. Diagram of: (a) Subdivision into Vertical Crack Strips for Purpose of Numerical Analysis; (b) Mesh Used for Calculating Compliance Functions of Plate Wedge

helps to carry the vertical load. The previous fracture analyses of this problem, except that of Dempsey et al. (1995a,b), could not capture the dome effect. The compressive stress above the part-through crack can be high enough to cause microcracking damage, which is manifested by a whitening of the ice surface seen from above (Frankenstein 1963). The dome effect is the reason why the cracks reach only through a part of the thickness (for loading up to the maximum load; after the peak, some cracks may penetrate through the whole thickness).

The partial opening of the radial cracks is a three-dimensional phenomenon. A detailed three-dimensional fracture mechanics analysis would be computationally expensive, if not intractable. In the present analysis, the vertical cracked cross section of the plate is subdivided by discrete nodes into narrow vertical strips. In each strip, the crack is assumed to propagate vertically and independently of the crack propagation in the adjacent strips. This simplification will require us to introduce some rule according to which the vertical crack in each strip initiates from the smooth surface of the plate. In reality, the crack front of course propagates horizontally from one vertical strip to the next and no new cracks initiate. This aspect is neglected in the present analysis. The resulting error may be expected to be small if most of the crack front edge is almost horizontal, which is certainly true since the radial crack is much longer than its vertical depth.

The weakening of the plate by a part-through crack will be modeled in terms of distributed nonlinear softening line springs, in the manner proposed by Okamura et al. (1972) and Rice and Levy (1972). In each infinitesimal vertical strip in the crack plane, the crack is assumed to grow vertically as a function of the bending moment and normal force in the same strip only, i.e., independently of the bending moments and normal forces in the adjacent strips. [This approximation is similar to replacing the foundation on an elastic half-space with the Winkler foundation; e.g., Bažant and Cedolin (1991).] By virtue of the line spring concept, the plate with radial cracks can still be analyzed as a two-dimensional problem. The effect of partial cracking in the plate is reflected by increased compliance, characterized by the line springs. In previous applications of the line spring concept (Rice and Levy 1972; Dempsey et al. 1995a,b), the shape of the depth profile of the part-through crack was assumed. In our approach, however, the depth profile will be considered as unknown and will be solved.

Denote by Δ and θ the additional in-plane circumferential relative displacement and relative rotation (about the radial ray) that is caused by the radial crack and is work-conjugate to N and M [Fig. 1(c)]; Δ and θ vary in an unknown way with the applied load and with the radial distance r. A positive bending moment is that which causes tension at the bottom surface of the plate, and a positive normal force is that which is tensile. According to the line spring concept

$$\Delta = \lambda_{11}N + \lambda_{12}M, \quad \theta = \lambda_{21}N + \lambda_{22}M \tag{2}$$

where $\lambda_{ij}(i, j = 1, 2)$ = compliances of the line springs

$$\lambda_{ij} = 2\,\frac{1 - \nu^2}{E}\int_0^b k_i(t)k_j(t)\,dt \tag{3}$$

$k_i(i = 1,2)$, where k_1 = stress intensity factor in an infinitely long plate with a single-sided crack (or notch) of depth $b(r)$, loaded remotely by a unit force N; and k_2 = stress intensity factor of the same strip loaded remotely by a unit moment M. Approximate expressions for λ_{11} and λ_{22} are given by Tada et al. (1985). So one needs to deduce an approximate expression only for λ_{12}. This has been done by means of (3).

The degree of accuracy of the line spring model was clarified by Kuo et al. (1995). They showed that the stress intensity factors obtained by the line spring model closely approach those calculated by three-dimensional analysis as the ratio of the radial crack length to the vertical crack depth increases. They also showed that the stress intensity factors calculated by the line spring model are very accurate for part-through cracks for which the ratio of the radial crack length to the crack depth is large, which is the case for sea ice.

The additional relative rotation θ and horizontal displacement Δ calculated from (2) must be equal to the rotation and displacement calculated from the compliances of the plate wedge. This represents a crack compatibility condition that reads as follows:

$$\lambda_{21}(r)N(r) + \lambda_{22}(r)M(r) = C_{MP}(r)\,\frac{P}{n} - \int_0^a C_{MM}(r, r')M(r')\,dr' \tag{4}$$

$$\lambda_{11}(r)N(r) + \lambda_{12}(r)M(r) = -\int_0^a C_{NN}(r, r')N(r')\,dr' \tag{5}$$

where n = number of radial cracks of length a; $C_{MP}(r)$ = rotation of the plate at r due to a unit P; $C_{MM}(r, r')$ = rotation of the plate at r due to a unit moment acting on the crack surfaces at r'; and $C_{NN}(r, r')$ = circumferential displacement at r due to a unit normal force N at r'. The negative sign in front of the integrals is due to the fact that a positive force on the crack surfaces causes the crack to close.

The applied load P is related to the load-point displacement u by the equation

$$u = C_{PP}P + \int_0^a C_{PM}(r)M(r)\,dr \tag{6}$$

where $C_{PM}(r) = C_{MP}(r)$; and compliance $C_{PP} = u$ caused by loading the plate wedge alone with $P = 1$.

Due to symmetry, the compliance functions are calculated for a wedge plate representing one-half of the wedge between two radial cracks [Fig. 1(b)] of length a and depth $b(r)$; $b(r) > 0$ for $a_0 \leq r < a$, and $b(r) = 0$ for $r \geq a$ along the radial line with a crack. The possibility that the radial crack lengths might become unequal is not considered.

The compliance influence functions can be discretely represented by compliance matrices. They are solved numerically, e.g., by the finite-element method or finite-difference method. The integrals in (4) and (5) are then approximated by sums, and thus (4) and (5) yield a system of nonlinear algebraic equations.

CRITERIA FOR PLASTIC AND LINEAR ELASTIC FRACTURE MECHANICS (LEFM) STAGES OF CRACK GROWTH

In a discrete formulation with n nodes along the radial ray containing the crack, there are $3n + 1$ unknown variables—namely, the nodal values of M, N, and b, and the applied load P, with the load-point displacement u being specified. Eqs. (6), (4), and (5) yield $2n + 1$ discrete compatibility equations. To obtain the same number of discrete equations and unknowns, we need one more equation for each node. The necessary equation is the fracture criterion. Various types of the fracture criterion needed for various stages of the analysis are schematically represented in Fig. 1(d).

The condition for crack propagation in the LEFM stage [stage 3 in Fig. 1(d)] may be written as

$$K_I = K_f, \ (a_0 \leq r \leq a) \tag{7}$$

in which

$$K_I = k_1[b(r)]N(r) + k_2[b(r)]M(r) \tag{8}$$

and K_I = stress intensity factor; $K_f = \sqrt{E'G_f}$ = critical stress intensity factor (fracture toughness) of sea ice; G_f = fracture energy of ice; E, ν = Young's modulus and Poisson's ratio of ice; and $E' = E/(1 - \nu^2)$.

Initially, the ice plate is elastic [stage 1 in Fig. 1(d)]. The initiation of the vertical crack strips from the plate surface ($b = 0$) cannot be handled by LEFM. In general, one could introduce the cohesive crack model of Hillerborg type for the initiation of cracks (Bažant and Planas 1998). But that would be unnecessarily complicated because, as the computations confirm, the portion of the radial crack length in which the crack is in the cohesive (or plastic) state is very small, and the maximum depth to which a plastic crack reaches is only about $0.02h$. But when h is small ($h \leq 0.2$ m), the plate fails by a punch-through cone around the circular loaded area.

Therefore, we can adopt a simplified form of the cohesive crack model. We will base it on the assumption that, after reaching the tensile strength limit f_t' of ice, the crack grows as a plastic crack at yield limit as long as both M and N are below the values that correspond, according to LEFM [Fig. 1(d)], to the values of θ and Δ. Specifically, we assume in this simplified model that, in the plastic limit state, the stress distribution consists of a constant normal stress equal to strength f_t' over the entire crack length and a linearly distributed normal stress across the remainder of the cross section (the ligament). Thus, after taking into account the horizontal and moment equilibrium conditions, we find that the plastic stage of the crack [stage 2 in Fig. 1(d)] is characterized by

$$\sigma_M(b) + \sigma_N(b) = f_t' \tag{9}$$

in which

$$\sigma_M(b) = \frac{6M}{h(h + 2b)}, \quad \sigma_N(b) = \frac{N}{h - b} \tag{10}$$

Strictly adhering to the theory of plasticity, one would have to introduce for the plastic stage 2 a normality rule as the flow rule that determines the relation between the ratio λ/Δ and the ratio M/N. However, (9) and (10) imply a different relation between these two ratios, namely

$$\frac{\Delta}{\lambda} = \frac{\lambda_{11} + \lambda_{12}(M/N)}{\lambda_{21} + \lambda_{22}(M/N)} \tag{11}$$

which differs from the normality rule of plasticity. So, with the strict plastic formulation, the transition from the plastic stage 2 to the LEFM stage 3 would be very complicated. It would not occur for M and N simultaneously. One would have to distinguish various transitional stages, and if such transitional stages were ignored, the values of M and N would change from the plastic to the LEFM stage discontinuously, by jumps. Numerical convergence of the solution would then be difficult to achieve.

To circumvent the aforementioned problem, the following simplifying idea is proposed: The flow rule for a plastic crack is defined by LEFM. This means that the ratio λ/Δ is assumed to be given by (11), which is a nonassociated flow rule. With this expedient assumption, both M and N are guaranteed to transit from the plastic stage 2 to the LEFM stage 3 simultaneously and continuously, without jumps.

When $b = 0$, the limit value of the ratio in (11) for $b \rightarrow 0$ needs to be used because $\lambda_{ij} = 0$ in that case. However, to avoid calculations of this limit value, the crack depth b is immediately extended from 0 to depth $10^{-6}h$ as soon as the elastically calculated stress reaches the tensile strength f_t' of ice. With this simplifying assumption, (11) never needs to be used, because, for $b > 0$, it is embedded in the compliance condition (3). Thus, in computations, it suffices to use the LEFM compatiblity equations in (4) and (5) at all times through stages 1, 2, and 3. In stage 2, these equations are used in conjunction with the plastic limit state criterion in (9), and in stage 3 in conjunction with the LEFM criterion in (8). In this manner, a continuous variation of M and N from stage 2 to stage 3 is ensured.

The limit state conditions of plastic state and of brittle crack propagation in (9) and (8) may be jointly expressed as

$$\max[K_I - K_f, f_t' - \sigma_M(b) - \sigma_N(b)] = 0 \tag{12}$$

This criterion may be used for both stages 2 and 3.

The plasticization of a part of the thickness of the ice plate is a simple approximation for damage caused by microcracking. In experiments, the microcracking is visually manifested by whitening of the ice plate. The microcracks develop principally at the interfaces between the columnar ice crystals and at the voids filled by brine.

The problem of crack initiation in the vertical strips is different from that studied by Bažant et al. (1979), Li and Bažant (1994), and Li et al. (1995). The reader is also referred to Bažant and Cedolin (1991, section 12.6). In those studies, the focus was on the initial crack spacing. But here, for the vertical strips, the problem of their spacing does not arise. The crack strips open only along the same radial ray.

Development of a large in-plane compressive force can cause the crack strip to unload. The unloading first causes a reduction of the stress intensity factor K_I below the critical value K_f. As long as $0 < K_I < K_f$, the crack strip can neither grow nor shorten. This is labeled as stage 4. If the case $K_I = 0$ is attained, K_I cannot decrease any more and further unloading causes the crack surfaces to come into contact. Thus, the length of the opened portion of the crack strip diminishes, which is equivalent to negative fracture growth at $K_I = 0$. This is labeled as stage 5. Stages 4 and 5 were included in the computer program, but in the present computations they have never been encountered. The crack strips were found to grow all the way to the maximum load. But stages 4 and 5 would no doubt occur in postpeak loading, and of course for unloading (decreasing P). Another type of unloading criterion would have to be programmed if the unloading were to begin from the plastic stage (stage 2), but this case has never been encountered.

NUMERICAL SOLUTION OF ICE PLATE WITH PART-THROUGH RADIAL CRACKS

Before tackling the crack problem, the values of the compliances $C_{MP}(r)$, $C_{MM}(r, r')$, and $C_{NN}(r, r')$ are calculated for the nodes $i = 1, 2, \ldots n$ along the ray with the crack and are stored as matrices. If the load-point displacement u is specified, there are $3n + 1$ unknown quantities to be solved; they are the internal forces $M(r)$, $N(r)$ and the crack depths $b(r)$ at the nodes of the radial ray with the crack, and the applied load P. These unknowns can be solved from $3n + 1$ nonlinear algebraic equations consisting of (6), (4), (5), and (12). If the solution is found, the radial crack length a can be obtained from the location of the last node that is not in the elastic state (stage 1).

The aforementioned solution procedure can be used in an incremental loading approach, in which the load-point displacement is incremented in small steps. However, this solution procedure was found to converge very slowly, and the resulting load-deflection curves were not very smooth. The reason was an unsystematic representation of the radial crack length a, defined as the distance from the origin to the first node that is in the elastic state (stage 1). The main problem was the representation of a radial crack tip that lies somewhere between two nodes. The numerical model cannot capture the difference between the crack with a tip in the middle between two nodes and the crack with a tip very close to one of the nodes. This causes roughness in the calculated response.

The problem has been remedied by adopting the radial crack length a (or its dimensionless parameter $\alpha = a/L_0$) as the controlled variable, instead of the displacement u. This makes it possible to move the tip of the radial crack, lying at distance a, from one node to the next in each loading step. Thus, the crack length a is forced to take only values compatible with the mesh. This approach adds the load-point displacement u as an additional unknown in each loading step. But at the same time the value of b is prescribed as 0 at one of the nodes (the crack tip node). So the number of unknowns remains $3n + 1$. With this modification, the solution converges much faster and the computed response becomes smoother.

The system of $3n + 1$ equations, with the inequality criteria for the stages of all the crack strips, is highly nonlinear. An efficient way for solving such an equation system is the Levenberg-Marquardt nonlinear optimization algorithm (Levenberg 1944; Marquardt 1963). All the equations are written such that the right-hand sides are zero. If an approximate solution is substituted, the right-hand sides are not exactly zero. The optimization algorithm is used to minimize the sum of the squares of the right-hand sides of all the equations. This sum cannot be negative. Ideally, if this sum could be reduced to zero, the right-hand side of each equation would then be also zero and the solution would be exact. In practice, it suffices to reduce the sum to a sufficiently small positive value satisfying a specified tolerance, which ensures the right-hand sides of all the equations to be sufficiently small.

Attempting to solve this equation system right away for some specified value of a, one would not obtain a unique and physically correct solution, because the sum of squares of the right-hand sides of nonlinear equations has typically many local minima. The correct solution can be obtained only if a very good initial state, close to the correct solution, can be supplied as the input for the start of the iterations in the next step. Fortunately, the present problem belongs to a special class of problems in which the solution can be traced in small steps from an initial state (in this case, $a = 0$) for which the solution is known. The solution obtained for the crack tip at one node is used as the input of the initial estimate of the solution for the start of the iterations. If the nodal spacing is sufficiently small, the solution for the tip at the previous node provides a very good estimate for starting the iterations. When the convergence is too slow, one needs to diminish the spacing of the nodes, which amounts to reducing the loading steps.

The growth of radial cracks in a star pattern does not lead to a maximum load and postpeak softening. The deflection curve is always rising. As known from small-scale field experiments (Frankenstein 1963) and confirmed for thick plates by the present calculations, the maximum load is determined by the initiation of circumferential cracks [Fig. 1(b)]. We assume these cracks to initiate anywhere along the radial crack, and the initiation to be decided by the strength criterion. Therefore, after the iterations for each step converge, the values of the radial normal stresses σ_{rr} on top of the plate are calculated for each node. This is done on the basis of the deflection curvature $w_{,rr}$ along the radial ray and twist angle $w_{\theta r}$ along the θ arc (r = constant). These are calculated approximately by a second-order finite-difference formula from the nodal deflections w. During the finite-difference calculations of the elastic compliance matrices of an ice plate wedge, the influence matrices of the circumferential bending stresses are obtained as well. They include the curvatures in the radial direction of the wedge, $\mathbf{F}_{rr}$; the curvatures in the θ direction, $\mathbf{F}_{\theta\theta}$; and the twist curvatures, $\mathbf{F}_{\theta r}$, per unit value of the bending stress σ_M and the normal stress σ_N along the radial ray with the crack and the applied load P. Labeling the components corresponding to σ_M, σ_N, and P by superscripts M, N, and P, and grouping σ_{rr}, $\sigma_{\theta\theta}$, and $\sigma_{\theta r}$ for all the nodes on the radial ray into column matrices, we have

$$\boldsymbol{\sigma}_{rr} = \mathbf{F}^M_{rr}\boldsymbol{\sigma}_M + \mathbf{F}^N_{rr}\boldsymbol{\sigma}_N + \mathbf{F}^P_{rr}P \tag{13}$$

$$\boldsymbol{\sigma}_{\theta\theta} = \mathbf{F}^M_{tt}\boldsymbol{\sigma}_M + \mathbf{F}^N_{tt}\boldsymbol{\sigma}_N + \mathbf{F}^P_{tt}P \tag{14}$$

$$\boldsymbol{\sigma}_{\theta r} = \mathbf{F}^M_{tr}\boldsymbol{\sigma}_M + \mathbf{F}^N_{tr}\boldsymbol{\sigma}_N + \mathbf{F}^P_{tr}P \tag{15}$$

The maximum principal stress in the horizontal plane is $\sigma_I = [\sigma_{rr} + \sigma_{tt} + \sqrt{4\sigma_{tr}^2 + (\sigma_{rr} - \sigma_{tt})^2}]/4$. When the maximum value $\sigma_{I\max}$ among all the nodes on the crack line reaches or exceeds the strength limit f_t', the circumferential crack initiates.

Since the maximum load is decided by the strength criterion, one might think that there should be no size effect. But this is not the case, as the computations confirm. The reason is that the failure occurs only as a consequence of radial crack growth and the strength limit is attained only when the ratio $\alpha = a/L_0$ reaches a certain value, which tends to a constant as the plate thickness h is increasing. The attainment of a certain relative crack length α is decided by the energy release criterion of fracture mechanics. Hence the size effect.

CLOSING REMARK

In the present paper, the method of numerical fracture analysis of the problem has been formulated. The numerical calculations, their analysis, comparison with test results, the questions of scaling, and formulation of the conclusions will be the subject of the companion paper (Bažant and Kim 1998), which follows in this issue.

APPENDIX. REFERENCES

Adamson, R. M., Dempsey, J. P., DeFranco, S. J., and Xie, Y. (1995). "Large-scale in-situ ice fracture experiments—Part I: Experimental aspects." *Ice Mechanics—1995*, J. P. Dempsey and Y. D. S. Rajapakse, eds., ASME AMD, New York, 207, 107–128.

Bažant, Z. P. (1984). "Size effect in blunt fracture: Concrete, rock, and metal." *J. Engrg. Mech.*, ASCE, 110, 518–535.

Bažant, Z. P. (1992a). "Large-scale fracture of sea ice plates." *Proc., 11th IAHR Ice Symp.*, T. M. Hrudey, ed., IAHR, IAHR, Delft, The Netherlands, 991–1005.

Bažant, Z. P. (1992b). "Large-scale thermal bending fracture of sea ice plate." *J. Geophys. Res.—Oc.*, 97(C11), 17739–17751.

Bažant, Z. P. (1993). "Scaling laws in mechanics of failure." *J. Engrg. Mech.*, 119(9), 1828–1844.

Bažant, Z. P. (1995). "Scaling of quasibrittle fracture and the fractal question." *ASME J. Mat. and Technol.*, 117(Oct.), 361–367.

Bažant, Z. P. (1997a). "Scaling of quasibrittle fracture: Asymptotic analysis." *Int. J. Fracture*, 83(1), 19–40.

Bažant, Z. P. (1997b). "Scaling of quasibrittle fracture: Hypotheses of invasive and lacunar fractality, their critique and Weibull connection." *Int. J. Fracture*, 83(1), 41–65.

Bažant, Z. P., and Cedolin, L. (1991). *Stability of structures: Elastic, inelastic, fracture and damage theories*. Oxford University Press, New York.

Bažant, Z. P., and Chen, E.-P. (1997). "Scaling of structural failure." *Appl. Mech. Rev.*, 50(10), 593–627.

Bažant, Z. P., and Gettu, R. (1991). "Size effects in the fracture of quasibrittle materials." *Cold regions engineering, Proc., 6th ASCE Int. Spec., Conf.*, D. S. Sodhi, ed., ASCE, Reston, Va., 595–604.

Bažant, Z. P., and Kim, J. J. H. (1998). "Size effect in penetration of sea ice plate with part-through cracks. II: Results." *J. Engrg. Mech.*, ASCE, 124(12).

Bažant, Z. P., Kim, J. J. H., and Li, Y.-N. (1995). "Part through bending cracks in sea ice plates: Mathematical modeling." *Ice Mechanics—1995*, J. P. Dempsey and Y. Rajapakse, eds., ASME AMD, New York, 207, 97–105.

Bažant, Z. P., and Kim, J.-K. (1985). "Fracture theory for nonhomogeneous brittle materials with application to ice." *Proc., ASCE Nat. Conf. on Civ. Engrg. in Arctic Offshore—Arctic 85*, L. F. Bennett, ed., ASCE, Reston, Va., 917–930.

Bažant, Z. P., and Li, Y.-N. (1994a). "Penetration fracture of sea ice plate:

Simplified analysis and size effect." *J. Engrg. Mech.*, ASCE, 120(6), 1304–1321.

Bažant, Z. P., and Li, Y.-N. (1994b). "Penetration through floating sea ice plate and size effect: Simplified fracture analysis." *J. Engrg. Mech.*, ASCE, 120(7), 1304–1321.

Bažant, Z. P., Ohtsubo, R., and Aoh, K. (1979). "Stability and post-critical growth of a system of cooling and shrinkage cracks." *Int. J. Fracture*, 15, 443–456.

Bažant, Z. P., and Planas, J. (1998). *Fracture and size effect in concrete and other quasibrittle materials*. CRC Press, Boca Raton, Fla.

Bažant, Z. P., Xi, Y., and Reid, S. G. (1991). "Statistical size effect in quasi-brittle structures. I: Is Weibull theory applicable?" *J. Engrg. Mech.*, ASCE, 117(11), 2609–2622.

Bernstein, S. (1929). "The railway ice crossing." *Trudy Nauchno-Technicheskogo Komiteta Narodnogo Komissariata Putei*, Soobshchenniya, 84, Moscow (in Russian).

Black, M. S. (1975). "Ultimate strength of two-way concrete slabs." *J. Struct. Div.*, ASCE, 101(1), 311–324.

Braestrup, M. W., and Morley, C. T. (1980). "Dome effect in RC slabs: Elastic-plastic analysis." *J. Struct. Div.*, ASCE, 106, 1255–1062.

DeFranco, S. J., and Dempsey, J. P. (1990). "Crack growth stability in S2 ice." *Proc., 10th Int. IAHR Symp. on Ice*, IAHR, Delft, The Netherlands, 168–181.

Dempsey, J. P. (1989). "The fracture toughness of sea ice." *Ice/structure interaction*, S. Jones et al., eds., Springer-Verlag, New York, 109–145.

Dempsey, J. P. (1990). "Notch sensitivity of ice." *Proc., 1st Mat. Engrg. Congr.*, ASCE, Reston, Va., 2, 1124–1133.

Dempsey, J. P. (1996). "Scale effects on the fracture of ice." *The Johannes Weertmann Symp.*, R. J. Arsenault et al., eds., The Minerals, Metals and Mat. Soc. (TMS), Warrendale, Pa., 351–361.

Dempsey, J. P., Adamson, R. M., and Mulmule, S. V. (1995a). "Large-scale in-situ fracture of ice." *Proc., FraMCoS-2*, F. H. Wittmann, ed., AEDIFICATIO Publishers, D-79104, Freiburg, Germany.

Dempsey, J. P., Slepyan, L. I., and Shekhtman, I. I. (1995b). "Radial cracking with closure." *Int. J. Fracture*, 73(3), 233–261.

Desayi, P., and Kulkarni, A. B. (1977). "Load-deflection behavior of restrained R/C slabs." *J. Struct. Div.*, ASCE, 103(2), 405–419.

Frankenstein, E. G. (1963). "Load test data for lake ice sheet." *Tech. Rep. 89*, U.S. Army Cold Regions Res. and Engrg. Lab., Hanover, N.H.

Frankenstein, E. G. (1966). "Strength of ice sheets." *Proc., Conf. on Ice Pressures against Struct., Tech. Memorandum No. 92, NRCC No. 9851*, Laval Univ., Québec, PQ, Nat. Res. Council of Canada, 79–87.

Kerr, A. D. (1975). "The bearing capacity of floating ice plates subjected to static or quasi-static loads—A critical survey." *Res. Rep. 333*, U.S. Army Cold Regions Res. and Engrg. Lab., Hanover, N.H.

Kerr, A. D. (1996). "Bearing capacity of floating ice covers subjected to static, moving, and oscillatory loads." *Appl. Mech. Rev.*, 49(11), 463–476.

Kuo, C. H., Keer, L. M., and Cordes, R. D. (1995). "A note on the line spring solution for a part-through crack." *Int. J. Fracture*, 72, 191–195.

Levenberg, K. (1944). "A method for the solution of certain nonlinear problems in least-squares." *Quarterly Appl. Mathematics*, 2, 164–168.

Li, Y.-N., and Bažant, Z. P. (1994). "Penetration fracture of sea ice plate: 2D analysis and size effect." *J. Engrg. Mech.*, ASCE, 120(7), 1481–1498.

Li, Y.-N., Hong, A. N., and Bažant, Z. P. (1995). "Initiation of parallel cracks from surface of elastic half-plane." *Int. J. Fracture*, 69, 357–369.

Marquardt, D. W. (1963). "An algorithm for least-squares estimation of nonlinear parameters." *J. Soc. Industrial Appl. Mathematics*, 11, 431–441.

Mulmule, S. V., and Dempsey, J. P. (1997). "Stress-separation curves for saline ice using fictitious crack model." *J. Engrg. Mech.*, ASCE, 123(8), 870–877.

Mulmule, S. V., Dempsey, J. P., and Adamson, R. M. (1995). "Large-scale in-situ ice fracture experiments—Part II: Modeling aspects." *Ice Mechanics—1995*, J. P. Dempsey and Y. Rajapakse, eds., ASME AMD, New York, 207, 129–146.

Nevel, D. E. (1958). "The theory of narrow infinite wedge on an elastic foundation." *Trans., Engrg. Inst. of Canada*, 2(3).

Ockleston, A. J. (1958). "Arching action in reinforced concrete slabs." *Struct. Engrg.*, 36(6), 197–201.

Okamura, H., Watanabe, K., and Takano, T. (1972). "Applications of the compliance concept in fracture mechanics." *6th Nat. Symp. on Fracture Mech., Progress in flaw growth and fracture toughness testing. ASME Spec. Tech. Publ. No. 536*, ASME, New York, 423–439.

Park, R. (1964). "Ultimate strength of rectangular concrete slabs under short-term uniform loading with edges restrained against lateral movement." *Proc., Inst. of Civ. Engrs.*, 28, 125–150.

Park, R. (1965). "The lateral stiffness and strength required to ensure membrane action at the ultimate load of a reinforced concrete slab and beam floor." *Mag. Concrete Res.*, 17(50), 29–38.

Park, R., and Gamble, W. L. (1980). *Reinforced concrete slabs*. Wiley-Interscience Publishers, New York.

Rice, J. R., and Levy, N. (1972). "The part-through surface crack in an elastic plate." *J. Appl. Mech.*, 39, 185–194.

Slepyan, L. I. (1990). "Modeling of fracture of sheet ice." *Mech. of Solids*, 155–161.

Sodhi, D. S. (1995a). "Breakthrough loads of floating ice sheets." *J. Cold Reg. Engrg.*, ASCE, 9(1), 4–20.

Sodhi, D. S. (1995b). "Wedging action during vertical penetration of floating ice sheets." *Ice Mechanics—1995*, J. P. Dempsey and Y. Rajapakse, eds., ASME AMD, New York, 207, 65–80.

Tada, H., Paris, P. C., and Irwin, G. R. (1985). *Stress analysis of cracks handbook*. Del Research Corp., Hellertown, Pa.